25th ABCM International Congress of Mechanical Engineering
October 20-25, 2019, Uberlândia, MG, Brazil

COB-2019-0980
MICROSTRUCTURE AND MECHANICAL CHARACTERIZATION AND STRENGTH ASSESSMENT OF A HEAT-TREATED SELECTIVE LASER MELTED 300-GRADE MARAGING STEEL

Fábio F. Conde
Waldek W. Bose Filho
Department of Materials Engineering, University of Sao Paulo (USP), Av. Joao Dagnone, 1100 Jd. Sta Angelina, 13563-120, Sao Carlos, Brazil.
fabiofariaconde@gmail.com
waldek@sc.usp.br

Julián Escobar
Metallurgical and Materials Engineering, University of São Paulo, SP,10 Av.Prof. Mello Moraes 2463, 05508-030 São Paulo, SP, Brazil.
juliandescobar@gmail.com

André Tschiptschin
Metallurgical and Materials Engineering, University of São Paulo, SP,10 Av.Prof. Mello Moraes 2463, 05508-030 São Paulo, SP, Brazil.
antschip@usp.br

André L. Jardini
National Institute of Biofabrication (BIOFABRIS), Faculty of Chemical Engineering, State University of Campinas, Av. Albert Einstein 500, 13083-852 Campinas, SP, Brazil.
andre.jardini@gmail.com

João Pedro Oliveria
UNIDEMI, Departamento de Engenharia Mecânica e Industrial, Faculdade de Ciências e Tecnologia, Universidade Nova de Lisboa, 2829-516, Caparica, Portugal
jp.oliveira@fct.unl.pt

Julian A. Avila
UNESP – São Paulo State University, Campus of São João da Boa Vista, Av. Profª Isette Corrêa Fontão, 505, Jardim das Flores, 13876-750 - São João da Boa Vista, SP, Brazil.
julian.avila@unesp.br

Abstract. *Additive manufacture is a principle of building products by addition of materials rather than subtraction. The ultra-high strength steel Maraging 300, present a significant alloy addition and depict a martensitic matrix hardened by precipitation through aging treatment, depict good toughness/strength ratio. In the present work, a maraging 300 was processed by selective laser melting (SLM) and an investigation was carried out on mechanical properties and microstructural features. A post-heat treatment was applied aiming homogenization, grain refinement, precipitation of intermetallics compounds and martensite-to-austenite reversion. Microstructural characterization and mechanical properties assessment were conducted by electron backscattered diffraction and tensile tests, respectively.*

Keywords: *18 Ni; Maraging 300; additive manufacturing; selective laser melting.*

1. INTRODUCTION

Additive manufacturing (AM) has found space these days due to the high flexibility of production and sustainability, almost without material discard. Although almost no structural product has been used in service yet, many efforts have been made to understand AM complexities. AM is a technology used to produce objects adding layer-by-layer from a 3D CAD file (Singh and Singh 2017). Among the many categories, selective laser melting is a bed powder fusion process in which thermal energy selectively fuses regions of a powder bed (ASTM F2792 2013).

Maraging is an ultra-high strength steel grade and its name indicates the combination of a martensitic matrix hardened by precipitation during aging treatments (ROHRBACH and SCHMIDT 1990; ASM 1991; Decker, Eash, and Goldman 1962; Floreen 1968). Also, it was suggested that changes in ductility and tensile strength of this material are mainly governed by the formation of precipitates during aging, while reversion of γ-Fe plays a minor role (Casati et al. 2016). Nonetheless, some authors believe that reverted austenite is responsible for improving ductility (Raabe et al. 2009; M. M. Wang et al. 2015). According to Ooi, *et al*., the presence of reverted austenite is beneficial mostly by its capacity to increase the work hardening of maraging steel during tensile tests and ductility (Ooi et al. 2013). Sometimes the increase in ductility comes at the expense of mechanical strength (Viswanathan, Kishore, and Asundi 1996; Pardal et al. 2007; Ooi et al. 2013).

In the present work, the influences of the martensite-to-austenite reversion on mechanical properties after selective laser melting of a maraging 300 steel were investigated. Four different conditions were presented, the as-built and three more with subsequent heat treatments, including homogenization, tempering and aging. The as-built condition was evaluated by scanning electronic microscopy (SEM) and energy dispersive spectroscopy (EDS). The as-built condition and the heat-treated samples were evaluated by electron backscattered diffraction (EBSD) and tensile tests.

2. EXPERIMENTAL PROCEDURE

2.1. Alloy synthesis and heat treatments

A maraging 300 powder alloy was selective laser melted (SLM) using an EOS DMLS M280 machine with the processing parameters provided by the supplier (EOS GmbH and EOS 2011). A previous Argon purge was conducted in the chamber before SLM. The final product density was determined through the Archimedes principle, following the ASTM 962 standard (ASTM E962-17 2017).

As-built (AB) condition and three different thermal routes were explored according to Table 1. First, a simple aging cycle (HT1) was conducted as a baseline for comparison purposes, measuring the efficiency of the AM process in terms of mechanical strength. Two additional routes to evaluate the effect of homogenization upon an SLM component were studied and are described in Table 1.

Table 1. Applied heat-treatment on the SLMed maraging 300 steel.

Samples	Applied Heat Treatments		
	Homogenization	Intercritical	Aging
HT1	---	---	480 °C/3 h
HT2	820 °C/1 h + air cooling	610 °C/10 min + air cooling	480 °C/3 h
HT3	---	610 °C/30 min + air cooling	480 °C/3 h

2.2. Microstructural characterization

Chemical composition was measured by optical emission analysis in ann RL-4460 Thermo Fisher spectrometer while carbon and sulfur were analyzed by a LECO CS844 spectrometer. Microstructural characterization was conducted using an FEI Quanta 650 FEG SEM, coupled with an EDS and EBSD detector. The EBSD measurements were conducted at 20keV with a step size of 0.125 µm. EBSD data were processed using the HKL Channel 5 system from Oxford. A thin sample (~100 nm) of the AB condition was cut, prepared and analyzed using an SEM FEI Helios 660 focus ion beam (FIB). EDS measurements were conducted, in this thin sample, looking any precipitated intermetallics produced during SLM process. Besides, EDS compositional maps were conducted in the FIB´s sample using a JEOL 2100F FEG transmission microscope (TEM).

2.3. Mechanical properties

Rectangular samples of 60 mm in length were used to conduct tensile tests under the ASTM E8 (ASTM International and ASTM 2009) standard requirements. Tensile tests were conducted at room temperature, crosshead speed of 0.033 mm s^{-1} and a load cell with a maximum capacity of 100 kN.

3. RESULTS

3.1. Microstructural characterization in the as-built condition

A relative density of 99.19 ± 0.13 % was obtained after SLM with a chemical composition, according to Table 2.

Table 2. Chemical composition (wt. %) of maraging 300 alloy.

Ni	Co	Mo	Ti	Al	C	Mn	Si	V	Fe
18.3	9.2	5.15	0.51	0.056	0.004	0.05	0.11	0.15	Bal.

Figure 1 shows the microstructural topography of the AB material, evidencing a typical (Ji, Chen, and Chen 2018; Prashanth and Eckert 2017) weld pool tracks in Figure 1a and cellular morphology in Figure 1b, which is correlated to local strong compositional segregations. Its average hardness was 398 ± 3 HV.

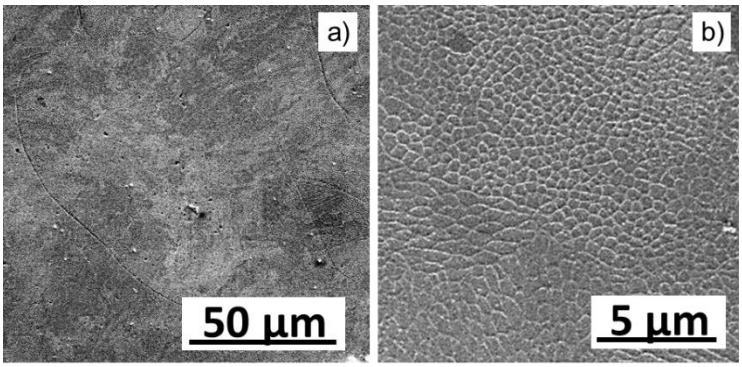

Figure 1. SEM microstructural characterization of the as-built condition, a) low magnification showing remaining weld pool tracks; and b) a high magnification image showing the cellular microstructural array, typical of AM building procedure. Samples were etched with 2 % nitric acid + ethanol.

During the SLM process, the laser melts the previously deposited powder at the surface and part of the already solidified material. As such, the solid material beneath the powder suffers reheating with gradually decaying temperature. The continuous thermal cycles in AM are an intrinsic feature of the process, resulting in a complex thermal history and microstructure. For age-hardening precipitation alloys, aging may occur during the build process due to the reheating cycles.

Figure 2 depicts the detailed microstructural analysis of the AB condition, starting for the FIB sample´s selection region in Figure 2.Figure 1a, samples extraction and lateral view in Figure 2.b. Figure 2.c evidence several spherical particles, some pointed with arrows, that after a compositional analysis, could not be possible to confirm their exact chemical composition. Moreover, elements such as Ti and Al often react with oxygen forming oxides on the SLM part during AM building process, as studied by TEM in a previous research (Gu 2015; Bodziak et al. 2019). Thus, it is suggested that these particles are oxides. Performing chamber sputtering with argon does not guarantee complete oxygen removal due to the lack of complete permeation between all powder particles. In addition, typical 18Ni steel precipitate could not be found through EDS analysis nor difference in the matrix composition were observed. SEM revealed the formation of a martensite lath mixed with polygonal grains in the as-built condition. Likewise, a high density of dislocation is depicted in Figure 2.d.

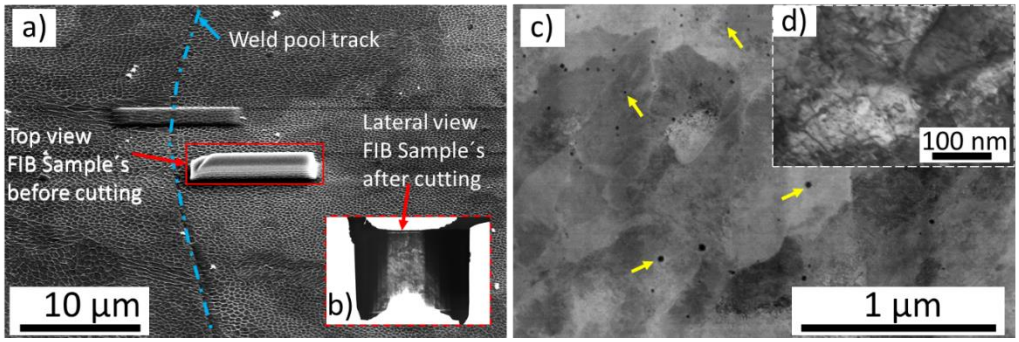

Figure 2. SEM images of AB FIB´s sample extraction: a) selection of the analysis region and b) lateral view of the sample after cutting. Microstructural details within the FIB´s sample: c) HAADF-STEM showing yellow arrows pointing out oxides, d) BF-STEM showing a high density of dislocation within the typical martensite microstructure.

3.2 Microstructural characterization after heat treatment

Inverse pole figure orientation maps (IPF) show the morphological information of the presented sample conditions, which is difficult to observe using light or electron microscopy. Figure 3.a evidenced the as-built condition, presenting a coarse-columnar microstructure. The efficiency of the homogenization temperature can be related to the degree of dissolution of the columnar structure towards a more refined and recrystallized one. At 820 °C, solidification pool and columnar features are still visible. However, grain growth and partial recrystallization occurred and is more clearly observed in Figure 3 c. A higher density of coarse new grains replaced the as-built fine grains.

The absence of a homogenization stage followed by aging (Figure 3.b) only resulted in the generation of new interfaces inside the existing microstructure, most likely due to an ongoing static recovery process accompanied by the interfacial segregation of alloying elements and secondary precipitation. Higher-resolution IPF maps, in the right upper corner of each condition, presented in better detail the evolution of the morphology of the martensitic laths. The microstructural refinement effect can be more clearly observed in the zoomed-in maps from Figure 3 d. This is caused by partial austenitization and reversion of martensite-to-austenite, resulting in the presence of clusters of fine inter-granular reverted austenite laths.

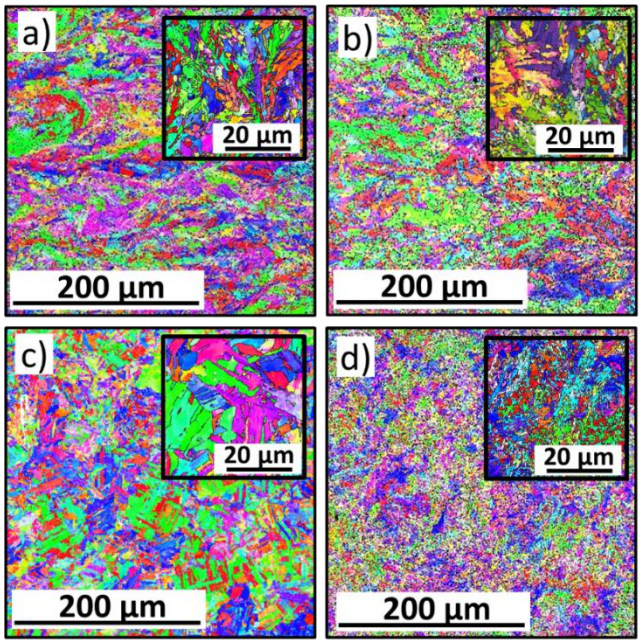

Figure 3. IPF maps of the lateral cross-section. Images revealed preservation of SLM morphology mainly from HT1 to HT3. Condition HT3 seemed to present a microstructure refinement through austenite reversion, and HT2 homogenization step acted recrystallizing the microstructure. a) as-built, b) HT1, c) HT2, and d) HT3.

3.3 Mechanical Properties

Table 3 presents the results of tensile tests. The as-built condition was tested for a base condition measurement. The highest tensile strength and lowest strain were obtained for samples after direct aging (HT1). The heat treatment routes HT2, HT3 presented lower yield and tensile strength than direct aged condition (HT1).

Table 3. Tensile mechanical test results for SLMed maraging 300-grade.

Condition	*Yield Stress (MPa) [0,2%]*	*Tensile Strength (MPa)*	*Strain (mm/mm) X10³*	*Austenite content (%)*
AB: SLM as-built	1192 ± 17	1233 ± 10	38± 1	0.2
HT1: SLM + 480°C/3 h	-	2097 ± 33	13 ± 7	0.5
HT2: SLM + 820 °C/1 h + 610 °C/10 min + 480°C/3 h	1596 ± 6,0	1657 ± 14	28 ± 1	5.8
HT3: SLM + 610°C/30 min + 480 °C/3 h	1411 ± 28	1440 ± 28	35 ± 1	17.2

4. DISCUSSION

Several studies contain the range of intermetallics precipitation for the 300-grade maraging steel analyzed by DSC and other techniques, showing low or no precipitation near the temperature of 600 °C (Guo, Sha, and Li 2004; Carvalho et al. 2013; Floreen 1968; ASM 1991), being aged typically between 420 and 580 °C. Conditions subjected to tempering at 610 °C promoted martensite-to-austenite reversion, but also the formation of coarse intermetallics, similar to some results reported in literature (Pardal et al. 2007; Casati et al. 2016; Kong and Liu 2018). Hence, a non-optimized condition is obtained for mechanical properties. Higher martensite-to-austenite reversion is obtained in this tempering, as also reported (Pardal et al. 2007). Subsequent aging at 480 °C after tempering at 610 °C may not result in any further increase of mechanical strength. A wise route for martensite-to-austenite reversion would be one avoiding any intermetallic precipitation.

Comparing HT2 and HT3, homogenization played an important role acting partially recrystallizing the microstructure, mainly erasing the prior fine grains resulted from the SLM process. Higher yield and tensile is achieved mainly by a shorter tempering time to promote martensite-to-austenite reversion. Therefore, subsequent aging resulted slightly higher tensile strength for HT2 than HT3. Moreover, higher strain ability is correlated to intermetallics precipitation and austenite content. HT3 presented higher austenite content and higher ductility in tensile tests.

The martensite-to-austenite reversion improved ductility in tensile tests. As reported in the literature, by increasing the amount of stable reverted austenite through aging at 600 °C, a continuous increase in elongation and toughness was observed along with the reduction in yield and tensile strength of samples (M. Wang et al. 2015). It has been reported almost a linear correlation of increase of total elongation with the increase of reverted austenite on a 350-grade maraging (Viswanathan, Kishore, and Asundi 1996). Viswanathan et al. reported similar results, an increasing amount of reverted austenite caused an increase of elongation with the decrease of yield and tensile strength. Beyond a threshold, toughness decreases, resulting in brittle behavior (Viswanathan, Dey, and Sethumadhavan 2005). Some results show only decrease of mechanical properties without any increase of ductility, being reported that strength and ductility are mainly governed by the effects of the precipitated intermetallics, as the martensite-to-austenite reversion plays a minor role (Casati et al. 2016).

5. CONCLUSIONS

- The as-built microstructure of an AM by SLM maraging 300-grade steel presented a non-homogeneous microstructure with low content of retained austenite, with no secondary precipitation according to the EDS analysis.
- Direct aging provided the highest strength condition with the smallest deformation to rupture due to preferential secondary precipitation.
- Martensite-to-austenite reversion promoted a slight increase of ductility and loss of tensile strength.
- Reverted austenite may be promoted by heat-treating the steel after SLM
- Tempering at 610 °C promotes martensite-to-austenite reversion

6. ACKNOWLEDGMENTS

We want to thank the Brazilian Nanotechnology National Laboratory (LNNano), CNPEM/MCTIC and Brazilian Synchrotron Light Laboratory (LNLS) CNPEM/MCTIC for the use of the SEM/EBSD and the XTMS beamline, respectively. Authors acknowledge FAPESP 2017/17697-5, FAPESP 2019/00691-0, FAPESP 2008/57863-0, FAPESP 2014/20844-1 and CNPq 130395/2017-0, Coordenação de Aperfeiçoamento de Pessoal de Nível Superior - Brasil (CAPES) - Finance Code 001, and the Portuguese foundation FCT - MCTES (UID/EMS/00667/2019) for their financial support. The chemical composition measurements were conducted at VILLARES METALS.

7. REFERENCES

ASM. 1991. “ASM Handbook - Heat Treatment.” *ASM Handbook* 4: 3470. https://doi.org/10.1016/S0026-0576(03)90166-8.

ASTM E962-17. 2017. “Standard Test Methods for Density of Compacted or Sintered Powder Metallurgy (PM) Products Using Archimedes ’ Principle.” *ASTM Book of Standards*, 1–7. https://doi.org/10.1520/B0962-17.2.

ASTM F2792. 2013. “F2792-12a - Standard Terminology for Additive Manufacturing Technologies.” *ASTM Book of Standards*, 10–12. https://doi.org/10.1520/F2792-12A.2.

ASTM International, and ASTM. 2009. “ASTM E8 Standard Test Methods for Tension Testing of Metallic Materials.” *ASTM Book of Standards*, no. C: 1–27. https://doi.org/10.1520/E0008.

Bodziak, Sabrina, Kassim S. Al-Rubaie, Luiz Dalla Valentina, Fernando Humel Lafratta, Edson Costa Santos, André Marcon Zanatta, and Yimeng Chen. 2019. “Precipitation in 300 Grade Maraging Steel Built by Selective Laser

Melting: Aging at 510 °C for 2 h." *Materials Characterization* 151 (September 2018): 73–83. https://doi.org/10.1016/j.matchar.2019.02.033.

Carvalho, Leandro Gomes de, Margareth Spangler Andrade, Ronald Lesley Plaut, Fabricio Mendes Souza, and Angelo Fernando Padilha. 2013. "A Dilatometric Study of the Phase Transformations in 300 and 350 Steels During Continuous Heating Rates." *Materials Research* 16 (4): 740–44. https://doi.org/10.1590/S1516-14392013005000069.

Casati, Riccardo, Jannis N Lemke, Ausonio Tuissi, and Maurizio Vedani. 2016. "Aging Behaviour and Mechanical Performance of 18-Ni 300 Steel Processed by Selective Laser Melting." *Metals* 6 (9): 218. https://doi.org/10.3390/met6090218.

Decker, R.F., J.T. T. Eash, and A.J. J. Goldman. 1962. "18% Nickel Maraging Steel.Pdf." *Transaction of ASM* 55: 58–76.

EOS GmbH, and EOS. 2011. "Material Data Sheet EOS Maraging Steel MS1." *EOS* 49 (0): 6. http://ip-saas-eos-cms.s3.amazonaws.com/public/1af123af9a636e61/042696652ecc69142c8518dc772dc113/EOS_MaragingSteel_MS1_en.pdf.

Floreen, S. 1968. "The Physical Metallurgy Maraging Steels." *METALLURGICAL REVIEWS*.

Gu, Dongdong. 2015. *Laser Additive Manufacturing (AM): Classification, Processing Philosophy, and Metallurgical Mechanisms*. *Laser Additive Manufacturing of High-Performance Materials SE - 2*. https://doi.org/10.1007/978-3-662-46089-4_2.

Guo, Z., W. Sha, and D. Li. 2004. "Quantification of Phase Transformation Kinetics of 18 Wt.% Ni C250 Maraging Steel." *Materials Science and Engineering A* 373 (1–2): 10–20. https://doi.org/10.1016/j.msea.2004.01.040.

Ji, Yanzhou, Lei Chen, and Long-qing Chen. 2018. *Understanding Microstructure Evolution During Additive Manufacturing of Metallic Alloys Using Phase-Field Modeling*. *Thermo-Mechanical Modeling of Additive Manufacturing*. 1st ed. Elsevier Inc. https://doi.org/10.1016/B978-0-12-811820-7.00008-2.

Kong, Hao Jie, and Chain Liu. 2018. "A Review on Nano-Scale Precipitation in Steels." *Technologies* 6 (1): 36. https://doi.org/10.3390/technologies6010036.

Ooi, S W, P Hill, M Rawson, and H K D H Bhadeshia. 2013. "Materials Science & Engineering A Effect of Retained Austenite and High Temperature Laves Phase on the Work Hardening of an Experimental Maraging Steel." *Materials Science & Engineering A* 564: 485–92. https://doi.org/10.1016/j.msea.2012.12.016.

Pardal, J. M., S. S.M. Tavares, M. P. Cindra Fonseca, M. R. Da Silva, J. M. Neto, and H. F.G. Abreu. 2007. "Influence of Temperature and Aging Time on Hardness and Magnetic Properties of the Maraging Steel Grade 300." *Journal of Materials Science* 42 (7): 2276–81. https://doi.org/10.1007/s10853-006-1317-8.

Prashanth, K G, and J Eckert. 2017. "Formation of Metastable Cellular Microstructures in Selective Laser Melted Alloys." *Journal of Alloys and Compounds* 707: 27–34. https://doi.org/10.1016/j.jallcom.2016.12.209.

Raabe, D., D. Ponge, O. Dmitrieva, and B. Sander. 2009. "Nanoprecipitate-Hardened 1.5 GPa Steels with Unexpected High Ductility." *Scripta Materialia* 60 (12): 1141–44. https://doi.org/10.1016/j.scriptamat.2009.02.062.

ROHRBACH, K, and M SCHMIDT. 1990. "ASM Handbook, Volume 1, Properties and Selection : Irons , Steels , and High Performance Alloys Section : Publication Information and Contributors Publication Information and Contributors." In *Metals Handbook*, v. 1:1618. https://doi.org/10.1002/jcb.240590830.

Singh, R., and S. Singh. 2017. "Additive Manufacturing: An Overview." *Reference Module in Materials Science and Materials Engineering*, 1–12. https://doi.org/10.1016/B978-0-12-803581-8.04165-5.

Viswanathan, U. K., G. K. Dey, and V. Sethumadhavan. 2005. "Effects of Austenite Reversion during Overageing on the Mechanical Properties of 18 Ni (350) Maraging Steel." *Materials Science and Engineering A* 398 (1–2): 367–72. https://doi.org/10.1016/j.msea.2005.03.074.

Viswanathan, U.K., R. Kishore, and M.K. Asundi. 1996. "Effect of Thermal Cycling on the Mechanical Properties of 350-Grade Maraging Steel." *Metallurgical and Materials Transactions A* 27A (12): 757–61.

Wang, M. M., C. C. Tasan, D. Ponge, A. Ch Dippel, and D. Raabe. 2015. "Nanolaminate Transformation-Induced Plasticity-Twinning-Induced Plasticity Steel with Dynamic Strain Partitioning and Enhanced Damage Resistance." *Acta Materialia* 85: 216–28. https://doi.org/10.1016/j.actamat.2014.11.010.

Wang, M, C C Tasan, D Ponge, A Dippel, and D Raabe. 2015. "ScienceDirect Nanolaminate Transformation-Induced Plasticity – Twinning-Induced Plasticity Steel with Dynamic Strain Partitioning and Enhanced Damage Resistance." *Acta Materialia* 85: 216–28. https://doi.org/10.1016/j.actamat.2014.11.010.

8. RESPONSIBILITY NOTICE

The authors are the only responsible for the printed material included in this paper.